第 26 卷第 12 期 无 机 化 学 学 报 Vol.26 No.12
2010 年 12 月 CHINESE JOURNAL OF INORGANIC CHEMISTRY 2266-2272

3,4-二甲氧基苯乙酸邻菲咯啉轻稀土配合物的合成、晶体结构、荧光光谱及热行为

余玉叶[1,3] 李花琼[1] 刘建风[1] 赵国良*[,1,2]
([1]浙江师范大学化学与生命科学学院,金华 321004)
([2]浙江师范大学行知学院,金华 321004)
([3]金华职业技术学院,金华 321007)

摘要: 合成了 3,4-二甲氧基苯乙酸邻菲咯啉轻稀土配合物:$[RE_2(DMPA)_6(phen)_2]$(RE=Ce (**1**),Pr (**2**),Nd (**3**),Eu (**4**);HDMPA=3,4-二甲氧基苯乙酸,$C_{12}H_{12}O_4$;phen=1,10-邻菲咯啉),用元素分析、红外光谱、热重分析对产物进行表征,用单晶 X-射线衍射方法测定了配合物 **3** 的晶体结构。配合物 $C_{84}H_{82}Nd_2N_4O_{24}$ (**3**)属于三斜晶系,$P\bar{1}$ 空间群,晶胞参数:a=1.242 06(9) nm,b=1.244 56(9) nm,c=1.477 88(11) nm,α=90.617(4)°,β=103.486(4)°,γ=116.870(3)°,晶胞体积:V=1.963 8(2) nm^3,晶胞内结构基元数 Z=1,分子量 M_r=1 820.02,电子数 F(000)=926,密度 D_c=1.539 g·cm^{-3},吸收系数 μ(Mo $K\alpha$)=1.389 mm^{-1}。测定了铕配合物的荧光光谱,荧光光谱表明,配合物显示了铕(Ⅲ)离子的特征发射,这表明配体将吸收的能量有效地转移给了中心离子,配体起到了很好的敏化作用。同时也测定了铕配合物的热分解情况,并利用 TG-DTG 曲线采用非等温积分法和微分法研究了热分解动力学机理。

关键词: 稀土配合物; 3,4-二甲氧基苯乙酸; 邻菲咯啉; 晶体结构; 荧光光谱; 热分解动力学机理
中图分类号: O641.33 **文献标识码**: A **文章编号**: 14001-4861(2010)12-2266-07

Synthesis, Crystal Structure, Luminescence Spectrum and Thermal Analysis of Light Rare Earth Complexes from 3,4-Dimethoxyphenylacetic Acid and 1,10-Phenanthroline

YU Yu-Ye[1,3] LI Hua-Qiong[1,2] LIU Jian-Feng[1,2] ZHAO Guo-Liang*[,1,2]
([1]*College of Chemistry and Life Sciences, Zhejiang Normal University, Jinhua, Zhejiang* 321004)
([2]*Zhejiang Normal University Xingzhi College, Jinhua, Zhejiang* 321004)
([3]*Jinhua College of Occupation and Technology, Jinhua, Zhejiang* 321007)

Abstract: Four light rare earth coordination polymers $[RE_2(DMPA)_6(phen)_2]$ (RE=Ce (**1**), Pr (**2**), Nd (**3**), Eu (**4**); HDMPA=3,4-dimethoxyphenylacetic acid, $C_{12}H_{12}O_4$; phen=1,10-phenanthroline) were synthesized and characterized by elemental analysis, IR, TG-DTG and X-ray crystallographically. The single-crystal X-ray diffraction studies demonstrated that complex **3** is crystallize in triclinic space group $P\bar{1}$ with a=1.242 06(9) nm, b=1.244 56(9) nm, c=1.477 88(11) nm, α=90.617(4)°, β=103.486(4)°, γ=116.870(3)°, V=1.963 8(2) nm^3, Z=1, M_r=1 820.02, F(000)=926, D_c=1.539 g·cm^{-3}, μ(Mo $K\alpha$)=1.389 mm^{-1} and formed 3D supramolecular architectures by hydrogen bonds and π-π stacking interactions. In all these complexes, the coordination number around RE(Ⅲ) center is nine. The fluorescence spectrum of complex **4** is investigated. It is indicated that the luminescence behavior of complex results from metal-centered emission, ligand can transfer the energy to the central metal efficiently and can sensitize the central metal. The thermal decomposition of complex **4** and its kinetic mechanisms and equations are studied under the non-isothermal integral and differential methods in air by TG-DTG curves. CCDC: 732322, **3**.

Key words: rare earth complex; 3,4-dimethoxyphenylacetic acid; 1,10-phenanthroline; crystal structure; fluorescence spectrum; kinetic mechanism of thermal decomposition

收稿日期:2010-04-30。收修改稿日期:2010-08-19。
*通讯联系人。E-mail:sky53@zjnu.cn
第一作者:余玉叶,女,46 岁,副教授;研究方向:功能配合物。

0 Introduction

Much atten tion has been focused on the design and synthesis of coordination polymers in supramolecular and materials chemistry, dues to their intriguing network topologies and promising applications in fields such as catalysis, ion exchange, gas storage, molecular magnets, optoelectronic devices, sensors, non-linear optics, lnminescence and so on[1-9]. The supramolecular architectures can be formed by non-covalent forces of their components, including coordination bonding, hydrogen bonding, aromatic π-π stacking interactions, electrostatic and charge-transfer attractions[6]. From the point of view of coordination chemistry, the interactions of ligands in a mixed-ligand complex can lead to a supramolecular formation[10].

It is well known that the coordination ability of aromatic carboxylic acids towards rare earth complexes has received considerable attention, dues to the strong coordination ability and varieties of the bridging modes of the carboxylate group with regard to the formation of extended frameworks[11-12]. Considering the high coordination number of lanthanide ions, ancillary ligands can be employed to occupy some coordination sites and prevent the interpenetration of frameworks. 1,10-Phenanthroline (phen), which has a rigid framework and two chelate positions is an appropriate ligand for lanthanide ions and can help construct stable supramolecular structures via C–H···O or C–H···N hydrogen bonds and π-π stacks[13-15]. In addition, phen can enhance the luminescent properties of lanthanide complexes due to the antenna effect. In this paper, we represent the syntheses and structure of four new three-dimensional coordination polymers $[RE_2(DMPA)_6(phen)_2]$ (RE = Ce, **1**; Pr, **2**; Nd, **3**; Eu **4**; HDMPA =3,4-dimethoxyphenylacetic acid). The luminescence and thermal properties of complex **4** are discussed.

1 Experimental

1.1 Materials and physical measurements

All reagents were of analytical grade and used without further purification. Elemental analysis was performed on C, H, N elemental analyzer, Elementar Vario EL Ⅲ. FTIR spectra were recorded on a Nicolet NEXUS 670 FTIR spectrophotometer using KBr discs in the range of 4 000~400 cm^{-1}. A Mettler Toledo thermal analyzer TGA/SDTA 851^e was used to carry out the thermoanalytical analysis with a heating rate of 10 ℃·min^{-1} from 30 to 900 ℃ in air atomsphere. The kinetic paramenters were obtained from the analysis of TG-DTG cures by integral and differential methods. Luminescence spectra in the solid state were recorded on an Edinburgh Instruments FS920 Steady State Fluorimeter.

1.2 Synthesis of the complexes

$RE(NO_3)_3 \cdot 6H_2O$ (1 mmol) in 10 mL ethanol was added dropwise into the solution of 3,4-dimet hoxyphenylacetic acid (3 mmol) and 1,10-phenanthroline (1 mmol) in absolute ethanol (20 mL) with continuous stirring. Solid power was precipitated when pH value of mixture solution was rose to 5~6 by adding NaOH (0.5 mol·L^{-1}). The products was filtered, washed by ethanol and dried.

[Ce $(DMPA)_3$phen$]_2$ (**1**): yellow, in yield 70% (based on $Ce(NO_3)_3 \cdot 6H_2O$). Elemental anal. calcd. for $C_{84}H_{82}Ce_2N_4O_{24}$(%): C, 55.69; H, 3.09; N, 4.56; Found(%): C, 55.54; H, 3.15; N, 4.48. IR (KBr, cm^{-1}): 1 515 (s, $\nu_{C=N(phen)}$), 1 592 (s, $\nu_{as\ COO^-}$), 1 421 (s, $\nu_{a\ COO^-}$), 850 (m, $\delta_{C\text{-}C(phen)}$),725 (w, $\delta_{C\text{-}H(phen)}$).

[Pr$(DMPA)_3$phen$]_2$ (**2**): light green, in yield 65% (based on $Pr(NO_3)_3 \cdot 6H_2O$). Elemental anal. calcd. for $C_{84}H_{82}Pr_2N_4O_{24}$(%): C, 55.64; H, 3.08; N, 4.55; Found (%): C, 55.17; H, 3.16 ; N, 4.45. IR (KBr, cm^{-1}): 1 515 (s, $\nu_{C=N(phen)}$), 1 600 (s, $\nu_{as\ COO^-}$), 1 424 (s, $\nu_{a\ COO^-}$), 849 (m, $\delta_{C\text{-}C(phen)}$), 725 (w, $\delta_{C\text{-}H(phen)}$).

[Nd $(DMPA)_3$phen$]_2$ (**3**): white, in yield 67%(based on $Nd(NO_3)_3 \cdot 6H_2O$). Elemental anal. calcd. for $C_{84}H_{82}Nd_2N_4O_{24}$(%): C, 55.43; H, 3.08; N, 4.54; Found(%): C, 55.56; H, 3.12; N, 4.47. IR (KBr, cm^{-1}): 1 515 (s, $\nu_{C=N(phen)}$), 1 601 (s, $\nu_{as\ COO^-}$), 1 424 (s, $\nu_{a\ COO^-}$), 848 (m, $\delta_{C\text{-}C(phen)}$), 726 (w, $\delta_{C\text{-}H(phen)}$).

[Eu$(DMPA)_3$phen$]_2$ (**4**): white, in yield 67% (based on $Eu(NO_3)_36H_2O$). Elemental anal. calcd. for $C_{84}H_{82}Eu_2N_4O_{24}$(%): C, 54.97; H, 3.05; N, 4.48; Found(%):

C, 54.78; H, 3.03 ; N, 4.42. IR (KBr, cm^{-1}): 1 515 (s, $\nu_{C=N(phen)}$), 1 605 (s, $\nu_{as\,COO^-}$), 1 422 (s, $\nu_{a\,COO^-}$), 847 (m, $\delta_{C-C(phen)}$), 725 (w, $\delta_{C-H(phen)}$).

Single crystals of complex **3** suitable for X-ray diffraction were obtained from above filter solutions by slow evaporation of the solvent at room temperature after 3 weeks.

1.3 Single-crystal struture determination

Intensity data of the complex **3** were measured at 296 K on a Bruker Smart APEX Ⅱ CCD diffractometer using graphite-monochromated Mo $K\alpha$ radiation (λ = 0.071 073 nm). Structure was solved by direct methods using SHELXS-97[16] and refined on the F^2 by full-matrix least-square method with SHELXL-97[17]. All non-hydrogen atoms were refined anisotropically. Hydrogen atoms were placed in geometrically calculated positions and refined by using a riding mode. Experimental details for X-ray data collection are presented in Table 1, and the selected bond lengths and angles are listed in Table 2.

CCDC: 732322, **3**.

Table 1 Crystal data and details of the structure determination for complex 3

Empirical formula	$C_{84}H_{82}N_4Nd_2O_{24}$	D_c / ($g\cdot cm^{-3}$)	1.539
Formula weight	1 820.02	Absorption coefficient / mm^{-1}	1.389
Temperature / K	296(2)	Crystal size/mm	0.474×0.173×0.091
Crystal system	Triclinic	Crystal color	Colorless
Space group	$P\bar{1}$	F(000)	926
a / nm	1.242 06(9)	Reflections collected	26 694
b / nm	1.244 56(9)	Unique reflections	6 916
c / nm	1.477 88(11)	Reflections observed ($I>2\sigma(I)$)	6 528
α / (°)	90.617(4)	θ_{min}, θ_{max} / (°)	1.94, 25.00
β / (°)	103.486(4)	R_1, wR_2 ($I>2\sigma(I)$)	0.027 1, 0.068 3
γ / (°)	116.870(3)	R_1, wR_2 (all data)	0.031 6, 0.070 6
V / nm^3	1.963 8(2)	Goodness-of-fit (on F^2)	1.091
Z	1	$\Delta\rho_{max}$, $\Delta\rho_{min}$ / ($e\cdot nm^{-3}$)	724, –459

Table 2 Selected bond distances (nm) and angles (°) for complex 3

Nd1-O7	0.240 33(19)	Nd1-O3	0.252 2(2)	Nd1-N2	0.262 4(2)
Nd1-O11	0.243 2(2)	Nd1-O8A	0.256 27(19)	Nd1-N1	0.268 6(2)
Nd1-O12A	0.243 4(2)	Nd1-O7A	0.259 6(2)	Nd1-Nd1A	0.399 32(4)
Nd1-O4	0.246 5(2)				
O7-Nd1-O12A	75.92(7)	O11-Nd1-O8A	77.96(7)	O4-Nd1-N2	86.02(8)
O7-Nd1-O11	74.69(7)	O4-Nd1-O8A	145.24(7)	O3-Nd1-N2	71.61(8)
O12A-Nd1-O11	137.12(7)	O3-Nd1-O8A	142.02(7)	O8A-Nd1-N2	76.52(7)
O7-Nd1-O4	88.42(8)	O7-Nd1-O7A	74.05(7)	O7A-Nd1-N2	123.17(7)
O12A-Nd1-O4	80.25(8)	O12A-Nd1-O7A	71.04(7)	O7-Nd1-N1	151.81(7)
O11-Nd1-O4	128.92(7)	O11-Nd1-O7A	71.31(7)	O12A-Nd1-N1	77.06(7)
O7-Nd1-O3	76.17(7)	O4-Nd1-O7A	149.13(7)	O11-Nd1-N1	132.35(7)
O12A-Nd1-O3	124.52(7)	O3-Nd1-O7A	140.99(7)	O4-Nd1-N1	79.20(7)
O11-Nd1-O3	76.97(7)	O8A-Nd1-O7A	50.21(6)	O3-Nd1-N1	113.68(7)
O4-Nd1-O3	52.08(7)	O7-Nd1-N2	142.96(8)	O8A-Nd1-N1	66.09(7)
O7-Nd1-O8A	123.26(7)	O12A-Nd1-N2	138.47(8)	O7A-Nd1-N1	104.44(7)
O12A-Nd1-O8A	93.12(7)	O11-Nd1-N2	80.62(8)	N2-Nd1-N1	61.87(8)

Symmetry code: A: 1–x, 1–y, –z.

2　Results and discussion

2.1　IR spectra

The broad absorption band at 3 451 cm^{-1} due to the hydroxy group and 1 718 cm^{-1} ($\nu_{C=O(-COOH)}$) in the IR spectra of the free ligand (HDMPA) disappears in the corresponding complexes. Two absorbption peaks at 1 592~1 607 ($\nu_{as\,COO^-}$) and 1 421~1 428 cm^{-1} ($\nu_{a\,COO^-}$) appears, showing coordination of the carboxylate oxygen atoms with the central RE(Ⅲ) ion[18]. However, three bands in the free phen ligand occurring at 1 560 cm^{-1} due to C=N stretching, 853 ($\delta_{C\text{-}C}$) and 739 cm^{-1} ($\delta_{C\text{-}H}$) are found shifted to lower frequency, viz., 1 516, 847~850, and 725~726 cm^{-1}, supports the coordination of nitrogen atoms of phen in complexes[19].

2.2　Structure of complex 3

The structure of complex **3** is described in detail. As shown in Fig.1, $[Nd_2(DMPA)_6(phen)_2]$ is a binuclear complex with Nd1…Nd1A separation of 0.399 32(4) nm and a center of symmetry. Its molecular structure consists of two Nd(Ⅲ) ions, six $DMPA^-$ anions and two phen ligands. Nd(Ⅲ) is nine-coordinated and surrounded by two nitrogen atoms from a phen molecule, seven carboxylate oxygen atoms from four 3,4-dimethoxyphenylacetic ligands ($DMPA^-$). The Nd-O bond distances range from 0.240 33(19)~0.259 6(2) nm, all of which are within the range of those observed for other nine-coordinated Nd (Ⅲ) complexes with oxygen donor ligands[20-21]. The Nd-N bond distances are 0.268 6(2) and 0.262 4(2) nm, which are similar to those in nine-coordinate complex[22].

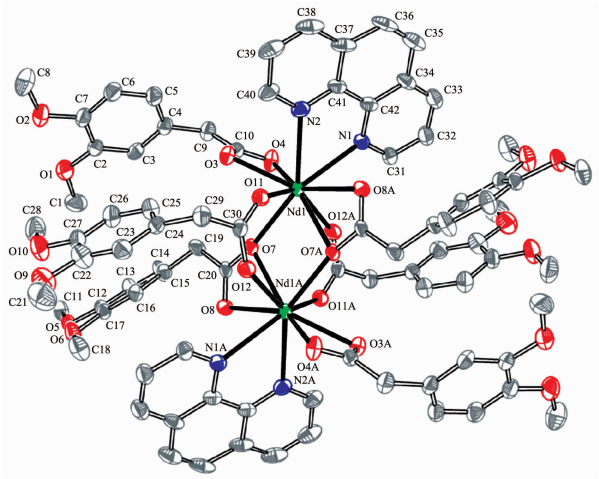

Symmetriy code: A: 1−*x*, 1−*y*, −*z*

Fig.1　ORTEP view of the complex **3** with thermal ellipsoids shown at the 30% level

The coordination geometry of Nd(Ⅲ) atom can be described as a distorted monocapped square antiprism (Fig.2). And the two symmetric Nd(Ⅲ) square antiprisms share a common edge, which is the band between O7 and O7A The coordinated atoms N2, O4, O7 and O11 form a similar square plane with a mean deviation of 0.014 46 nm. N1, O7A, O8A and O12A determined another square plane and its mean deviation from plane is 0.007 51 nm. The two plan possesse a dihedral angle of 2.659(43)°. To complete the coordination environment of the Nd center, atom O3 is located as the cap.

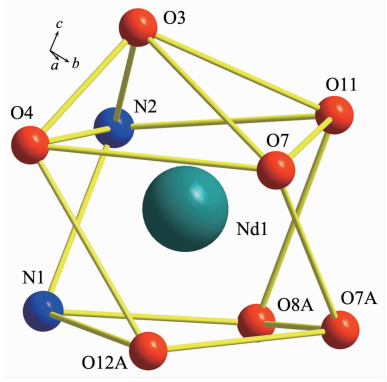

Symmetriy code: A: 1−*x*, 1−*y*, −*z*

Fig.2　Environment of Nd(Ⅲ) in complex **3**

It should be noteworthy that there exist three types of coordination modes of 3,4-dimethoxyphenylacetic ligand in this complex: (i) Chelating bidentate (Fig.3a): around each Nd (Ⅲ), there is one $DMPA^-$ ligand takes this mode through two O atoms from the carboxyl group.

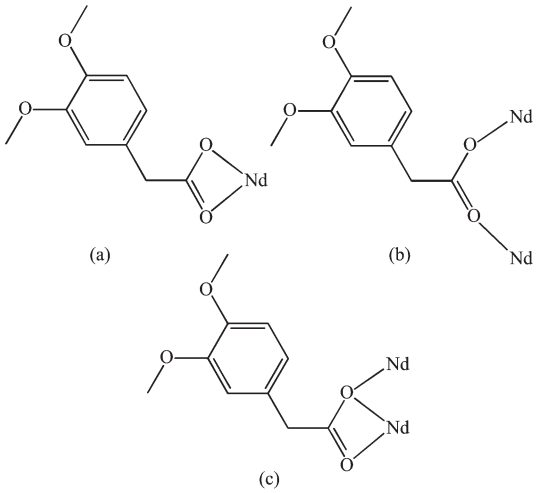

Fig.3　Coordination modes of $DMPA^-$ ligand in complex **3**

The Nd-O distances are 0.246 5(2) and 0.252 2(2) nm, respectively. (ii) Bridging bidentate (Fig.3b): there are two symmetric $DMPA^-$ ligands bridging the two Nd centers though O11 and O12 with distances of 0.243 4(2) and 0.243 2(2) nm. (iii) Bridging tridentate (Fig.3c): a $DMPA^-$ ligand bidentates with one Nd ion with O7 and O8 from carboxyl group and simultaneously bands to the other Nd ion with O7. The distances are 0.256 27(19), 0.259 6(2) and 0.240 33(19) nm for Nd1-O8A, Nd1-O7A and Nd1-O7, respectively. These are apparently important for rational design and constitution of new framework structures[22].

In addition, there are no classical hydrogen bonds in the crystal structure, presumably because good hydrogen bond donors are absent. In complex **3**, the most significant intermolecular interactions are C–H⋯O hydrogen bonds and weak π-π aromatic interactions along the c axis exist between the 1,10-phenanthroline molecules of neighboring sheets.

2.3 Thermogravimetric analysis

The processes of thermal decomposition of the title complexes are very similar and three stages of decomposition are observed, the residue are rare earth oxides. No weight loss was observed of complexes before 200 ℃, indicating that there are not any small molecular of solvent. Complex **4** was discussed as an example, its TG-DTG curves were shown in Fig.4. The TG degradation of the compound reveals three decomposition stages, as predicted by the DTG curve. The first stage stars from 206 ℃ to 312 ℃ with a mass loss 30.92% which corresponds to the loss of 3 mol $DMPA^-$ of permole complex (theoretical loss is 30.73%). The second stage decomposition temperature is in the range

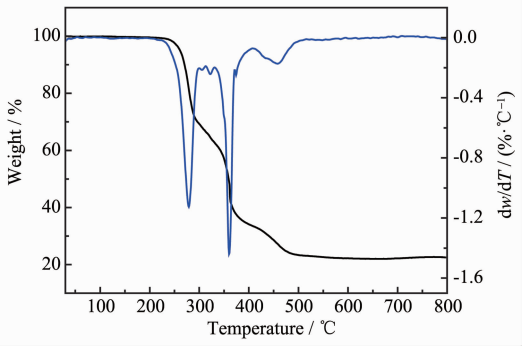

Fig.4 TG-DTG curves of complex **4**

of 312~408 ℃ with a mass loss 30.99% which corresponds to the loss of another 3 mol $DMPA^-$ (theoretical loss is 30.73%). The third stage of decomposition in the 408~586 ℃ temperature range, in which 2 mol phen was removed with a mass loss of 19.51% (theore-tical loss is 19.61%). The residue weights 18.58% corresponds to values calculated for Eu_2O_3 18.93%. This result is in good accordance with the composition of the complex.

The kinetic mechanisms of thermal decomposition of three stages of the complex **4** were discussed by integral and differential methods. The kinetic equations were confirmed by methods of non-isothermal ACHAR[23]:

$$\ln\frac{g(\alpha)}{T^2}=\ln\frac{AR}{\beta E}-\frac{E}{RT} \quad (1)$$

and non-isothermal COATS-REDFERN[24]:

$$\ln\frac{\mathrm{d}\alpha}{\mathrm{d}T}\cdot\frac{1}{f(\alpha)}=\ln\frac{A}{\beta}-\frac{E}{RT} \quad (2)$$

The basic parameters of α, T and $\mathrm{d}\alpha/\mathrm{d}T$ are obtained by the TG-DTG curves. Substitute the different mechanism functions $g(\alpha)$ and $f(\alpha)$ into equation (**1**) and (**2**) respectively. Plotting $\ln\frac{g(\alpha)}{T^2}$ and $\ln\frac{\mathrm{d}\alpha}{\mathrm{d}T}\cdot\frac{1}{f(\alpha)}$ vs $\frac{1}{T}$ respectively and using a linear least squares method, the linear regression of the data in each thermal decomposition process is carried out. Kinetic parameters E, A and linear correlation coefficients r[25] are calculated. When the values of E and A obtained by the two methods are approximately equal, the linear correlation coefficient is better and the values of E and $\ln A$ accord with the universal law, it can be concluded that the relevant function is the probable thermal decomposition mechanism of the complex. For the first stage of decomposition of the complex, it can be suggested that the functions of the possible mechanism are $g(\alpha)=(1-\sqrt[3]{1-\alpha})^2$ and $f(\alpha)=\frac{3}{2}\sqrt[3]{(1-\alpha)^2}\cdot\frac{1}{1-\sqrt[3]{1-\alpha}}$. The decomposition reaction was governed by three-dimensional diffusion 2D3 (spherical symmetry). The kinetic equations of this process

are $\ln[\frac{2}{3}\cdot\frac{d\alpha}{dt}\cdot\frac{1-\sqrt[3]{1-\alpha}}{\sqrt[3]{(1-\alpha)^2}}]=\ln A-\frac{E}{RT}$ and $\ln\frac{(1-\sqrt[3]{1-\alpha})^2}{T^2}=\ln\frac{AR}{\beta E}-\frac{E}{RT}$. We found that the r values are much close to the value given by the integral and differential methods of the both stages. By using the expiatory effect expression $\ln A=aE+b$ (a, b are expiatory parameters) and integral kinetic parameters and dealing $\ln A$-E with linearity fitting by least squares fit, we can get a_1=4.595 9, b_1=3.830 1; a_2=4.609 6, b_2=24.831. So the expiatory effect expression of integral kinetics and differential kinetics are $\ln A_1$=4.595 9E_1+3.830 1; $\ln A_2$=4.609 6E_2+24.831.

Similiarly, the functions of the possible mechanism are $g(\alpha)=(\sqrt[3]{1+\alpha}-1)^2$, $f(\alpha)=\frac{3}{2}\cdot\sqrt[3]{(1+\alpha)^2}\cdot\frac{1}{\sqrt[3]{1+\alpha}-1}$ for the second stage and $g(\alpha)=\sqrt{\frac{1}{\sqrt[3]{1-\alpha}}-1}$, $f(\alpha)=\frac{3}{2}\cdot\sqrt[3]{(1-\alpha)^4}\cdot[(1-\alpha)^{-\frac{1}{3}}-1]^{-1}$ for the third stage. The decomposi-tion reaction was governed by three-dimensional diffusion 3D3 for the second stage and 4D3 for the third stage. The kinetic equations are $\ln[\frac{2}{3}\cdot\frac{d\alpha}{dt}\cdot\frac{\sqrt[3]{1-\alpha}-1}{\sqrt[3]{(1-\alpha)^2}}]=\ln A-\frac{E}{RT}$, $\ln\frac{(\sqrt[3]{1+\alpha}-1)^2}{T^2}=\ln\frac{AR}{\beta E}-\frac{E}{RT}$ for the second stage and $\ln[\frac{2}{3}\cdot\frac{d\alpha}{dt}\cdot\frac{\frac{1}{\sqrt[3]{1-\alpha}}-1}{\sqrt[3]{(1-\alpha)^4}}]=\ln A-\frac{E}{RT}$, $\ln\frac{\sqrt{\frac{1}{\sqrt[3]{1-\alpha}}-1}}{T^2}=\ln\frac{AR}{\beta E}-\frac{E}{RT}$ for the third stage. The expiatory effect expression of integral kinetics and differential kinetics are $\ln A_1$=5.282 9E_1+2.875 2, $\ln A_2$=5.298 3E_2+30.55 for the second stage; $\ln A_1$=6.020 7E_1+9.736 8, $\ln A_2$=6.096 1E_2+37.505 for the third stage respectively.

2.5 Fluorescence spectrum of complex 4

The fluorescence spectrum of complex **4** at room temperature was studied using an excitation wavelength of 395 nm. Its photoluminescence spectra is given in Fig.5. As can be seen, the main emission band is suppressed followed by the strong red luminescence, characteristics of the $^5D_0\rightarrow{}^7F_J$ (J=0, 1, 2, 3, 4) emission bands of the Eu^{3+} ion[26]. The emission at 580, 593, 620, 688 and 697 nm corresponds to $^5D_0\rightarrow{}^7F_0$, $^5D_0\rightarrow{}^7F_1$, $^5D_0\rightarrow{}^7F_2$, $^5D_0\rightarrow{}^7F_3$ and $^5D_0\rightarrow{}^7F_4$ transitions, respectively. It has been observed that the emission band of the $^5D_0\rightarrow{}^7F_J$ peaks also give an idea about the coordination environment. For example, a (2J+1) splitting is observed in the emission band for a single type of environment (coordination environment and site symmetry) around the metal ion. In the present case, only one emission band has been observed in the $^5D_0\rightarrow{}^7F_0$ degenerate transition around 580 nm. This indicates that the Eu^{3+} ion occupies only one of the three crystallographic sites. The emission at 593 nm corresponds to $^5D_0\rightarrow{}^7F_1$ transition, which is induced by magnetic dipole moment and is fairly insensitive to the coordination environment[26]. The emission at 620 nm corresponds to the $^5D_0\rightarrow{}^7F_2$ transition, which is induced by the electric dipole moment and also sensitive to the environment. The intensity of I ($^5D_0\rightarrow{}^7F_2$) is much stronger than I ($^5D_0\rightarrow{}^7F_1$), indicates a lower symmetry level of the coordination environment of the Eu^{3+} occupied site[27].

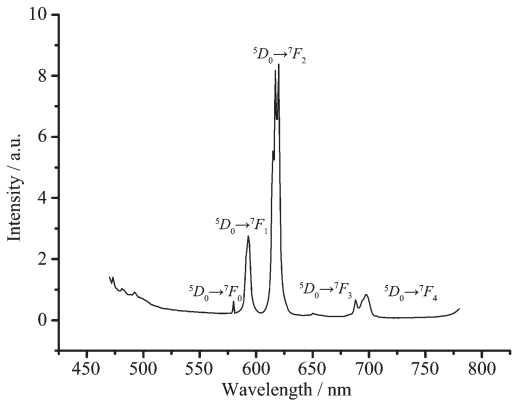

Fig.5　Luminescence spectra of complex **4**

References:

[1] Leadbeater N E, Marco M. *Chem. Rev.*, **2002**,**102**(10):3217-3274

[2] Eddaoudi M, Moler D B, Li H, et al. *Acc. Chem. Res.*, **2001**, **34**(4):319-330

[3] Yagi O M, OKeeffe M, Ockwig N W, et al. *Nature*, **2003**,**423**: 705-714

[4] Kitagawa S, Kitaura R, Noro S. *Angew Chem Int Ed*, **2004**,**43**:

2334-2375

[5] Ocwig N W, D-Friedrichs O, OKeeffe M, et al. *Acc. Chem. Res.*, **2005**,**38**(3):176-182

[6] Moulton B, Zawarotko M J. *Chem. Rev.*, **2001**,**101**:1629-1658

[7] HUANG Ling(黄 玲), HUANG Chun-Hui(黄春晖). *Acta Chimica Sinica*(*Huaxue Xuebao*), **2000**,**58**(12):1493-1498

[8] LI Zhe-Feng(李哲峰), ZHANG Hong-Jie(张洪杰). *Chem. J. Chin. Univesities*(*Gaodeng Xuexiao Huaxue Xuebao*), **2008**, **29**(12):2597-2608

[9] YANG Jun(杨 军), WANG Jia-Chen(王甲辰), LIU Xiang-Sheng(刘向生), et al. *J. Chin. Rare Earth Soc.*(*Zhongguo Xitu Xuebao*), **2007**,**25**(Suppl.):77-81

[10]Lehn J M. *Angew. Chem. Int. Ed.*, **1988**,**27**(1):89-112

[11]Li Y, Zheng F K, Liu X, et al. *Inorg. Chem.*, **2006**,**45**(16): 6308-6316

[12]Fiedler T, Hilder M, Junk P C, et al. *Eur. J. Inorg. Chem.*, **2007**,**2**:291-301

[13]González-Baró A C, Pis-Diez R, Piro O E, et al. *Polyhedron*, **2008**,**27**(2):502-512

[14]Liu C B, Yu M X, Zheng X J, et al. *Inorg. Chim. Acta*, **2005**, **358**(9):2687-2696

[15]WU Xiao-Shuo(吴小说), LI Xia(李 夏). *Chinese J. Inorg. Chem.*(*Wuji Huaxue Xuebao*), **2008**,**24**(10):1621-1625

[16]Sheldrick G M. *SHELXS*-97, *Program for the Solution of Crystal Structures*, University of Götingen, Germany, **1997**.

[17]Sheldrick G M. *SHELXL*-97, *Program for the Refinement of Crystal Structures*, University of Götingen, Germany, **1997**.

[18]Gao H L, Yi L, Zhao B, et al. *Inorg. Chem.*, **2006**,**45**(15): 5980-5988

[19]Udai P S, Shalu T, Chokhe L S, et al. *J. Chem. Soc., Dalton Trans.*, **2002**:4464-4470

[20]Evans W J, Giarikos D G, Ziller J W. *Organometallics*, **2001**,**20**:5751-5758

[21]Niu SY, Yang Z Z, Yang Q H, et al. *Polyhedron*, **1997**,**16**(10): 1629-1635

[22]Shi X, Zhu G S, Wang X H, et al. *Cryst. Growth & Des.*, **2005**, **5**(1):207-213

[23]LI Yu-Zeng(李余增). *Thermal Analysis*(热分析). Beijing: Tsinghua University Press, **1987**.

[24]ZHANG Jian-Jun(张建军), WEI Hai-Yu(魏海玉), REN Zhi-Qiang(任志强). *Chinese J. Inorg. Chem.*(*Wuji Huaxue Xuebao*), **2001**,**17**(2):279-284

[25]TANG Ding-Xing(唐定兴), ZHAO Yun(赵 芸). *Chin. J. Appl. Chem.*(*Yingyong Huaxue*), **2003**,**20**(8):760-763

[26]Sabbatini N, Guardigli M, Lehn J M. *Coord. Chem. Rev.*, **1993**,**123**(1/2):201-228

[27]Thirumurugan A, Natarajan S. *J. Mater. Chem.*, **2005**,**15**:4588 -4594